Award Number: 06HQGR0159

Physical Constraints on Upper Bound Ground Velocity

Final Report

July 30, 2008

Seok Goo Song, Arben Pitarka, and Paul Somerville
(Contact Email: Seok_Goo_Song@URSCorp.com)

URS Group, Inc.
566 El Dorado Street
Pasadena, CA 91101-2560
Tel: (626) 449-7650
Fax: (626) 449-3536

Abstract

This project addresses **Element 1 – National and Regional Earthquake Hazards assessments** – of the Research Priorities for FY 2006, specifically, the need in EP to **"Evaluate the variability and upper bound limit of ground motion distribution used in probabilistic seismic hazard assessment."** Current ground motion prediction models assume an unbounded lognormal distribution of random variability in ground motion level. The unbounded distribution in probabilistic seismic hazard analysis leads to very large ground motion levels at low annual probabilities of exceedance. The objective of this project is to investigate source characteristics of finite faults, in particular, spatial correlation between key source parameters, that will control the intensity and variability of near-field ground motions, and to seek constraints on high levels of ground velocity due to source complexities and their coherence. Our focus is solely on source effects that affect ground velocities, which are typically controlled by ground motions having periods of 1 second and longer. At these periods, we are usually able to match the amplitudes and waveforms of strong motion recordings using synthetic seismograms, and hence derive kinematic rupture models of the source. Wave propagation effects and site effects such as triplications, caustics, and focusing effects, which can potentially cause large amplification of ground motions, are excluded from the scope of the project.

We investigated spatial coherence between earthquake source parameters by analyzing both kinematic and dynamic rupture models. The coherence is considered not only at the same point (zero offset), but in neighboring areas (nonzero offset), by adopting the coherence analysis method of 2D spatial data, which is commonly used in Geostatistics. We examined kinematic rupture models for two major strike-slip events, the 1999 Izmit, Turkey, and 1992 Landers, California, earthquakes and one synthetic dynamic rupture model, constructed with simplified stress distributions. Our results show that earthquake slip has a significant level of correlation with temporal source parameters such as rupture velocity, peak slip rate, and slip duration (or rise time) in both kinematic and dynamic rupture models. This coherence pattern show interesting decay patterns as the nonzero offset distance increases. Many interesting features of earthquake source characteristics, such as directional effects of earthquake rupture, can be captured by spatial coherence analysis, in particular, in 2D spatial coherence analysis. For instance, horizontally and vertically elongated slip distributions tend to generate horizontally and vertically elongated coherence patterns, respectively, which implies that slip asperity geometry may affect characteristics of temporal source parameters. Also the correlation maximum can be located away from the zero offset, i.e., large slip may generate faster rupture velocity ahead of the current rupture front rather than at its current location, which may be an important characteristic with respect to rupture directivity effects.

This new approach will enable us to consider the spatial coherence in earthquake source characterization and help us to handle constructive and destructive interference in dynamic wave-fields, and consequently understand upper bound limits of ground motions. This type of coherence analysis may have potential for understanding earthquake source characteristics effectively in the framework of spatial coherence, and for developing effective source modeling tools for strong ground motion prediction.

1. Introduction

Earthquake rupture is a complex mechanical process that can be modeled by solving the elasto-dynamic equations with appropriate stress conditions and friction laws applied on a fault. Since kinematic motions on the fault are derived from a single mechanical process of earthquake rupture, kinematic source parameters are expected to correlate with each other to account for the mechanical consistency of earthquake rupture. Near-field strong ground motion characteristics, in particular, its upper bound limits, are affected by the coherence of earthquake source parameters as we see, for example, in the directivity effect. We are, however, limited in our ability to produce physically self-consistent earthquake source models, and many factors are still poorly constrained in earthquake source modeling for strong motion prediction. Several studies have been done to investigate the spatial distribution patterns of earthquake slip and develop tools to produce possible slip distributions for scenario events (*Herrero and Bernard*, 1994; *Somerville et al.*, 1999; *Mai and Beroza*, 2002; *Lavallée and Archuleta*, 2003). Some approaches have also tried to combine the slip model with temporal source parameters (rupture velocity, slip rate, rise time, etc.) in a physically self-consistent way by using spontaneous dynamic rupture modeling or correlated random source models (*Guatteri et al.*, 2004; *Liu et al.*, 2006; *Song et al.*, 2007). They aim to develop effective source characterization methods that avoid inconsistencies between simulated source parameters, so we can simulate more realistic near-field ground motions. In order to tackle this issue more rigorously, we investigated the spatial coherence of both well-constrained kinematic rupture models and a synthetic dynamic rupture model, and tried to quantify the coherence that may be embedded in the kinematic motions of earthquake rupture.

2. Estimating spatial coherence

The main idea of this study is to consider the coherence between source parameters not only at the same point (zero offset), but in neighboring areas (nonzero offset), separated by a vector, **h**, as shown in Figure 2.1. By doing so, we expect to see many interesting features of the earthquake source process, in particular, how earthquake source parameters interact with one another in a 2D spatial domain during earthquake rupture. The spatial coherence between source parameters can be computed by the equations given below.

$$C(\mathbf{h}) = E\{(X(\mathbf{u}) - m_X)(Y(\mathbf{u}+\mathbf{h}) - m_Y)\} \tag{2.1}$$

$$\rho(\mathbf{h}) = C(\mathbf{h}) / (\sigma_X \sigma_Y)$$

The two random variables, X and Y, can be any source parameters such as slip, rupture velocity (V_r), peak slip rate (V_{max}), etc. m_X and m_Y are the means of X and Y, and σ_X and σ_Y are their standard deviations, respectively. $C(\mathbf{h})$ indicates co-variance between X specified at a position, **u,** and Y separated by a vector, **h**, from **u**. Its normalized variable, $\rho(\boldsymbol{h})$, is called a

"correlogram" (*Goovaerts*, 1997) and it enables us to quantify the spatial coherence between earthquake source parameters from given earthquake rupture models. All random variables used in this study are assumed to follow stationary distributions, so their mean and variance are the same at every point within a single distribution, and the co-variance between different variables depends only on the separation vector, **h**.

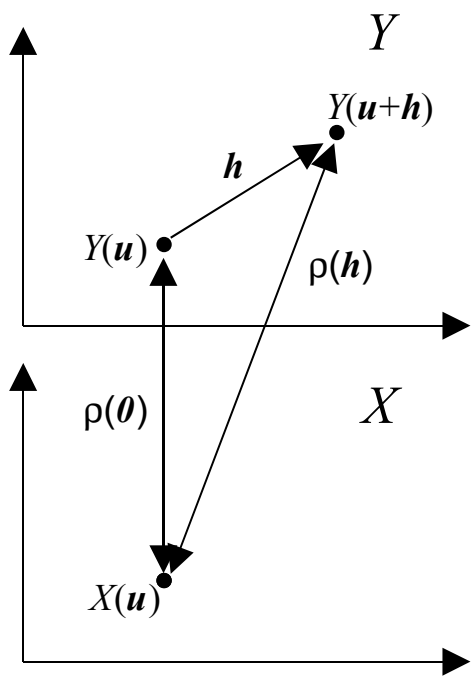

Figure 2.1. Schematic diagram showing the concept of the "correlogram," which indicates the correlation coefficient as a function of a separation vector, **h**. Since random variables *X* and *Y* are assumed to follow a stationary distribution, the correlation depends only on the separation vector, **h**, not on the specific location. A 1D correlogram, ρ(h), can be obtained by averaging ρ(**h**) over the same distance.

3. Spatial Coherence in Kinematic rupture models

Correlations between earthquake source parameters have been reported from kinematic source inversion studies and are expected from rupture dynamics. For instance, large slip is observed to drive faster rupture velocity (*Hernandez et al*., 1999). But methods for rigorously investigating and quantifying the coherence have not yet been introduced. We believe that the correlogram, introduced above, is a robust tool to resolve the problem. In order to estimate possible spatial coherence that may be embodied in currently available earthquake source models, we chose two large strike-slip events, the 1999 Izmit, Turkey, and 1992 Landers,

California, earthquakes. Both events were intensively studied by numerous researchers and various rupture models have been produced from many different inversion methods and data sets. We selected only kinematic rupture models obtained from multiple data sets, i.e., by joint inversion, including geodetic (GPS and InSAR), seismic (teleseismic and near-field strong ground motion), and surface offset. We believe that kinematic rupture models are more stably constrained by the multiple data sets, reducing trade-offs between source parameters in the inversion. Although *Bouchon et al.* (2002) used only near-field strong motion data, we decided to include their model for comparison purposes and it is also interesting to look at it since it suggests super-shear rupture during the event.

Extra care has been taken in extracting each source parameter since each finite source inversion adopted different fault parameterizations and inversion schemes. Source parameters are directly extracted from rupture models if they are estimated in the inversion. Then the remaining parameters were computed carefully from given estimates. We used instantaneous (local) rupture velocity in the analysis by taking the inverse of the spatial derivative of rupture time distribution as shown in the equation below.

$$V_r = 1/|\nabla t(x, y)| \tag{3.1}$$

If a multiple time window method is used in the inversion, average slip for each 1 second time interval is computed and the amount of slip in the time window that contains maximum slip is considered peak slip rate. In this way we can obtain more stable estimates of the peak slip rate. Slip duration (rise time) is computed by dividing slip by peak slip rate. The source parameters were low-pass filtered (cut-off λ = 10 km) since kinematic rupture models have limited spatial resolution, and interpolated on a 1 km by 1 km grid spacing for consistency in the analysis. We computed the spatial coherence only in the areas releasing large strain energy, i.e., large slip, and initial nucleation zones and areas near fault boundaries are excluded as well. Extracted key source parameters for the Izmit and Landers events are shown in Figures 3.1 and 3.2, respectively.

The correlogram analysis of the kinematic rupture models shows that a significant level of spatial coherence exists between earthquake source parameters, not only at zero offset, but in neighboring areas. Furthermore their decay patterns as a function of a separation vector, **h**, or separation distance, h, show interesting features about earthquake source characteristics, ingrained in the 2D spatial domain. For the Izmit event (Figure 3.3 (a)), slip correlates significantly with rupture velocity and peak slip rate, but not with rise time. Slip correlates strongly with peak slip rate and rise time for the Landers event, but not with rupture velocity (Figure 3.3 (b)). It is interesting that two different rupture models for a single event share source parameters that show significant correlations. For the Landers event, the decay patterns of both models, except those of slip vs. rupture velocity that shows low correlations, look similar, while the correlations (circle) from *Delouis et al.* (2002) decay faster than those (triangle) from *Bouchon et al*. (2002) for the Izmit event. Since we have analyzed a limited number of rupture models (2 events, 4 rupture models), it is difficult to extract certain common features of the decay pattern for correlated parameters. But it is worthwhile to note that strong correlations between earthquake source parameters exist even at the non-zero

offset (h > 0) and their different decay patterns may contain some important characteristics of earthquake rupture.

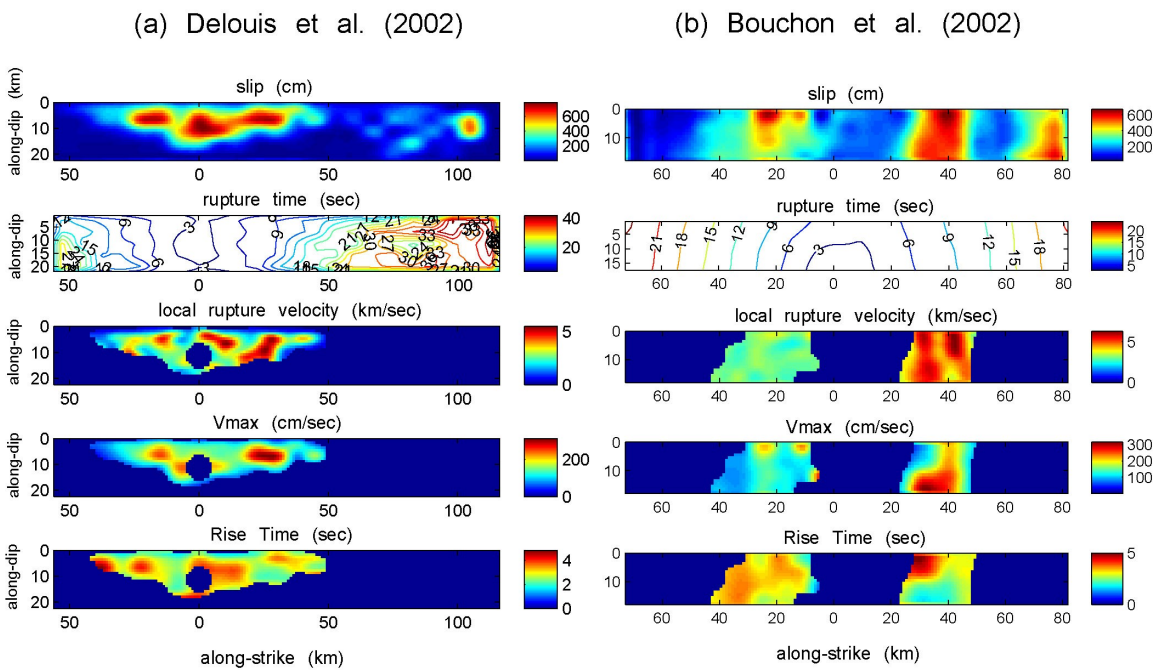

Figure 3.1. Source parameters used in the analysis for the 1999 Izmit, Turkey, earthquake: (a) Delouis et al. (2002), (b) Bouchon et al. (2002). All source parameters are interpolated on a 1 km by 1 km grid spacing for the analysis after low-pass filtering with cut-off wavelength, □ = 10 km. Initial nucleation zones and small slip areas whose slip is smaller than its mean slip as well as areas near fault boundaries are excluded in the analysis as indicated in dark blue in the three temporal source parameters in the bottom three plots.

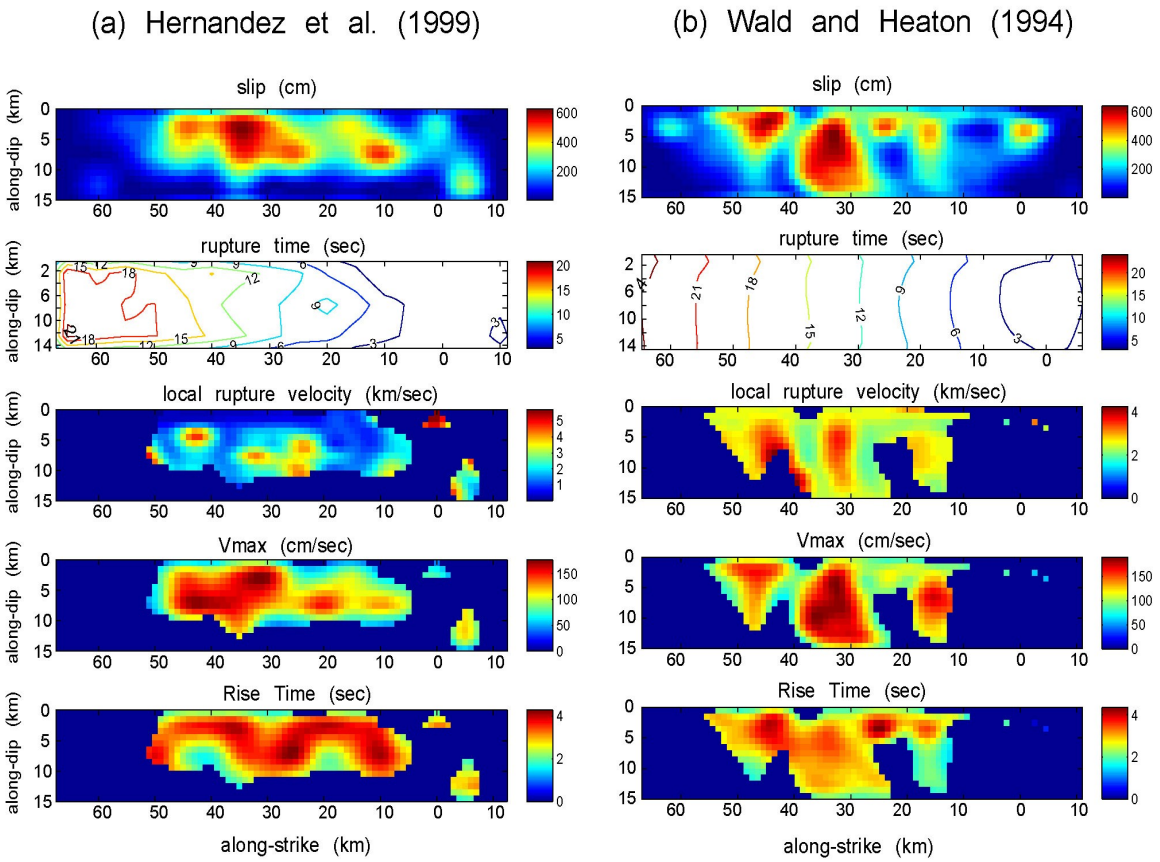

Figure 3.2. Source parameters used in the analysis for the 1992 Landers, California, earthquake: (a) Hernandez et al. (1999), (b) Wald and Heaton (1994).

Directional effects of earthquake rupture are captured in the 2D coherence analysis (Figures 3.4 and 3.5). For instance, horizontally and vertically elongated slip distributions tend to generate horizontally and vertically elongated coherence patterns, respectively, which implies that slip asperity geometry may affect characteristics of temporal source parameters. Also note that the correlation maximum can be located away from the zero offset, i.e., large slip may generate faster rupture velocity ahead of the current rupture front rather than that at its current location (Figure 3.4 (a)). This feature cannot be detected by coherence analysis and implemented in earthquake source modeling if we consider the coherence only at the zero offset. The coherence between slip and rise time from one rupture model (*Wald and Heaton*, 1994) for the Landers event shows an eye-ball shaped pattern (Figure 3.5 (b)). It may result from a local barrier ahead of the rupture front reducing the correlation in the along-strike direction quickly as the separation distance increases. Otherwise it shows a horizontally elongated pattern due to the shallow fault boundary on the bottom (Figure 3.4 (a)).

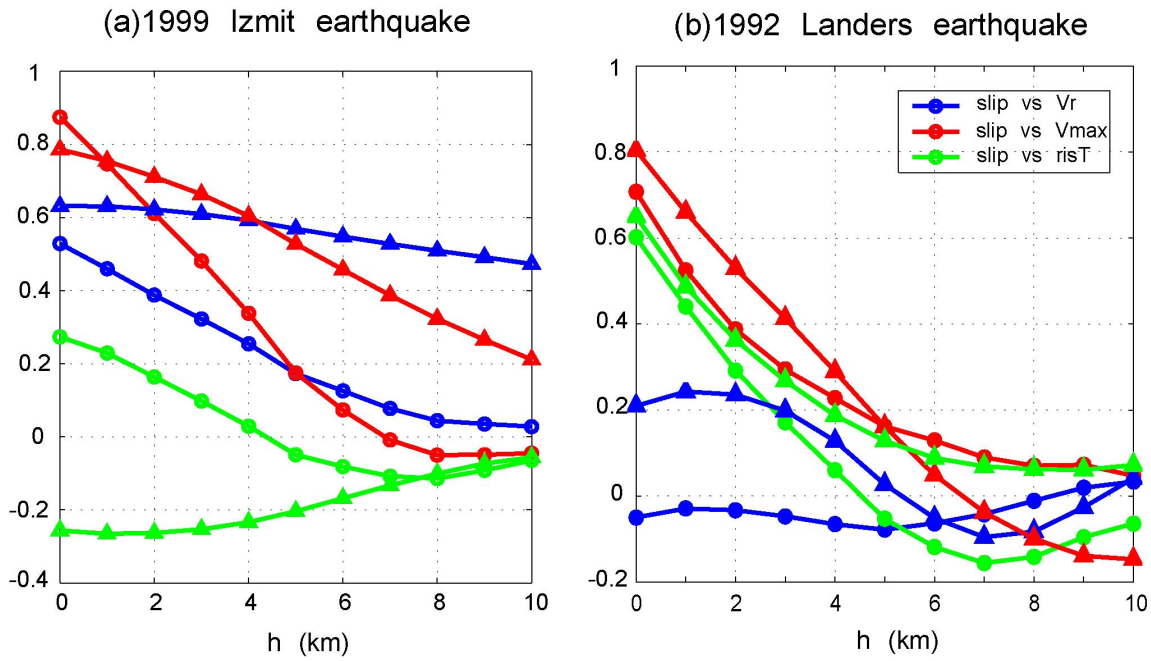

Figure 3.3. 1D spatial coherence between slip and other source parameters from different kinematic rupture models for two large strike-slip events: (a) 1999 Izmit earthquake (circle: Delouis et al. (2002), triangle: Bouchon et al. (2002)), (b) 1992 Landers earthquake (circle: Hernandez et al. (1999), triangle: Wald and Heaton (1994)). Note that the decay patterns and slopes of the different parameters are different depending on the rupture model and the event as the separation distance, *h*, increases.

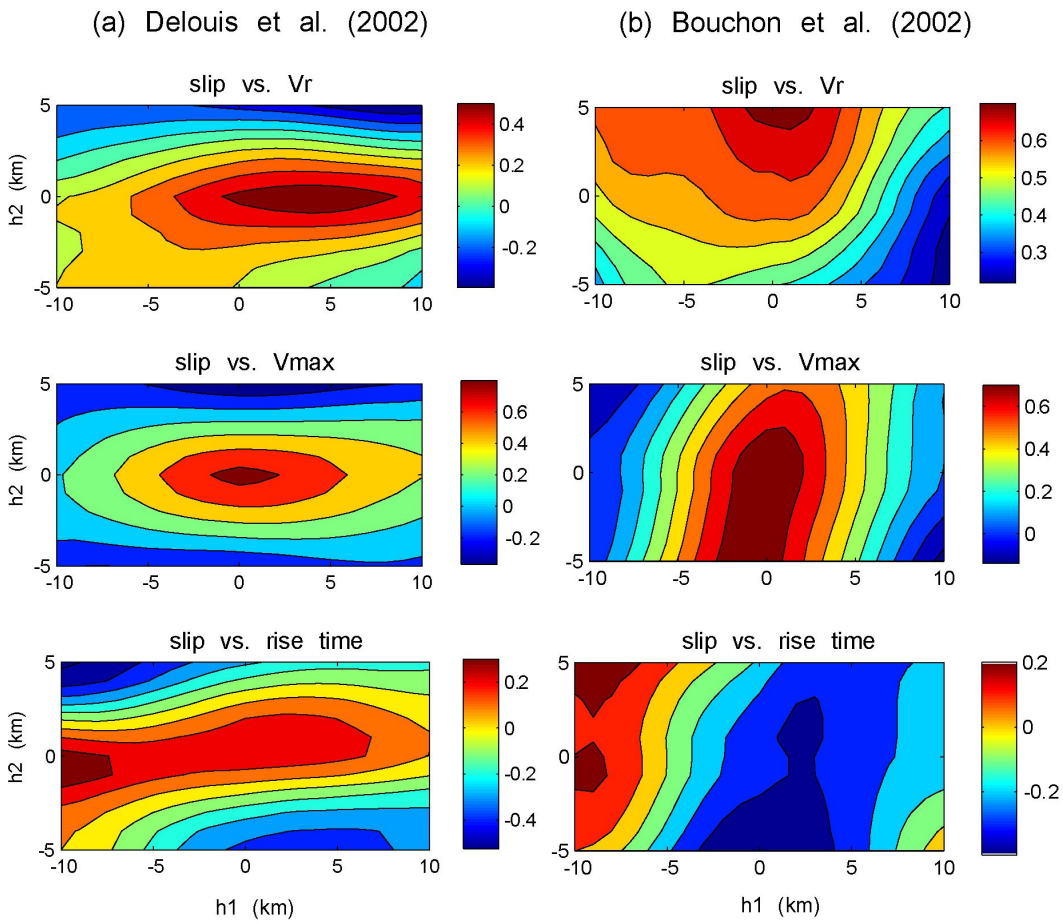

Figure 3.4. 2D spatial coherence for the 1999 Izmit, Turkey, earthquake: (a) Delouis et al. (2002), (b) Bouchon et al. (2002). Note that the 2D spatial coherence is elongated horizontally or vertically depending on the rupture model. Note also the shifted maximum observed in the correlation between slip and Vr on the top left panel.

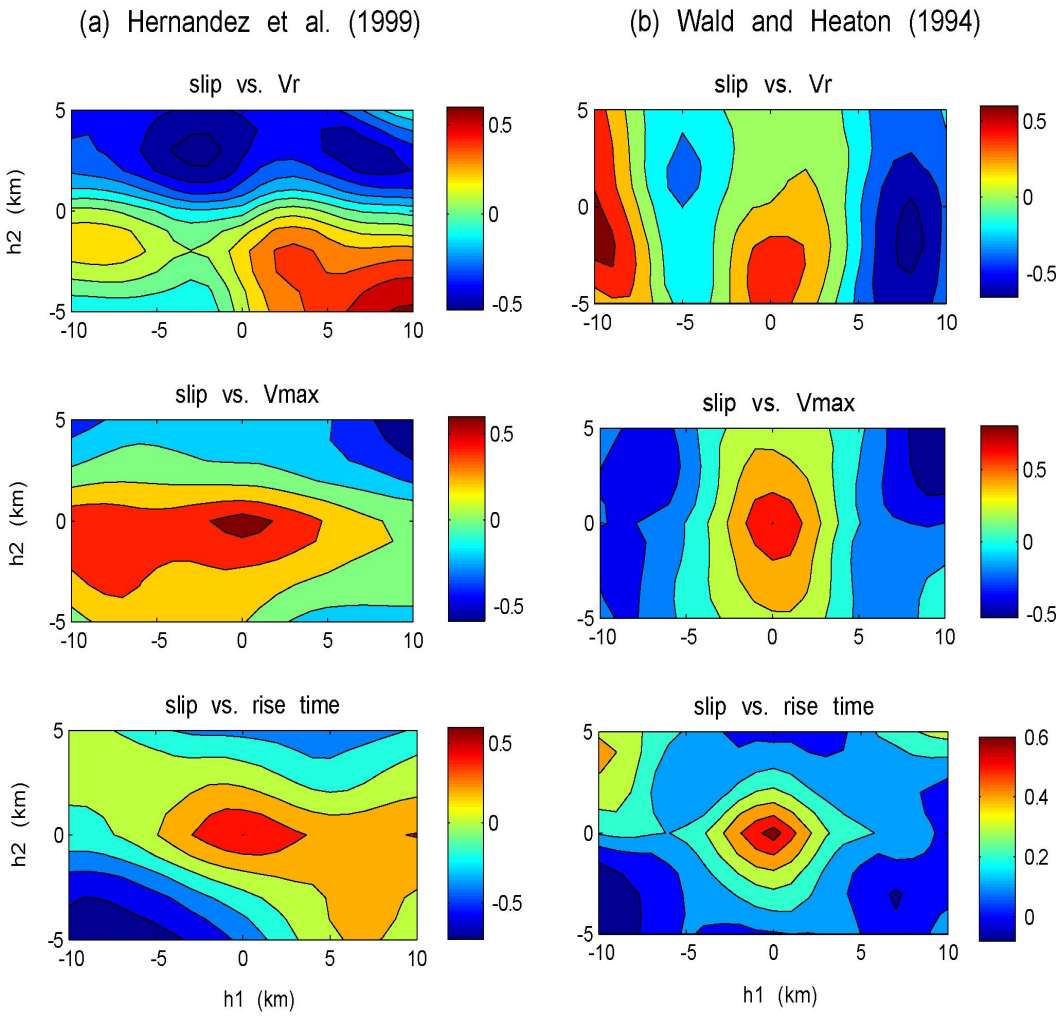

Figure 3.5. 2D spatial coherence for the 1992 Landers, California, earthquake: (a) Hernandez et al. (1999), (b) Wald and Heaton (1994). Similar patterns are observed for this event as we have seen for the Izmit event. Also note the eye-ball shaped coherence pattern in the bottom right panel that might be produced because of a local barrier ahead of a rupture front.

4. Spatial Coherence in Dynamic Rupture Models

Kinematic rupture models developed with different data sets and inversion methods show obvious dissimilarities even for the same event. This deviation between rupture models is often used to raise questions about the reliability of estimated rupture models (*Beresnev*, 2003; *Mai et al.*, 2007). The coherence patterns analyzed in the previous section also show some differences between two rupture models for a single event although the analysis was performed in a low wave-number domain ($\lambda > 10$ km). Since no explicit constraints on the coherence in the kinematic fault motions are applied in the inversion, intrinsic features of the coherence that may exist in earthquake rupture do not have to be embedded in the estimated models as long as the models fit the data satisfactorily. Thus it is difficult to determine which

coherence pattern is preferred for each event in the coherence analysis of kinematic rupture models. One possible improvement is to investigate dynamic rupture models of those events. Earthquake rupture can be formulated as a dynamically running shear crack on a frictional interface embedded in a linearly elastic continuum (*Andrews*, 1976; *Day*, 1982). Kinematic motions derived from dynamic rupture models should not only fit the data, but contain coherence if required by shear crack propagation. The main disadvantage of the dynamic models, however, is the lack of information to realistically parameterize the friction model and the state of stress in the Earth.

We tested the spatial coherence with a synthetic dynamic rupture model constructed with simplified stress distributions. The dynamic model was originally constructed by *Dalguer et al*. (2008) to investigate the characteristics of surface and buried dynamic rupture models. Four square-shaped asperities are embodied in a long and thin background rupture area (M_w 7.5, 100 km (along-strike) by 20 km (along-dip)). Key source parameters extracted from the rupture model, using the same approach as in the kinematic rupture model, are shown in Figure 4.1. We can see the effect of asperities in this dynamic rupture model both in terms of rupture velocity acceleration and high peak slip rate as the rupture front passes by each asperity. This effect is clearly captured in the 2D spatial coherence analysis (Figure 4.3), although the correlation maximum between slip and rupture velocity is shifted in the forward rupture direction by about 8 km while the maximum between slip and peak slip rate is located near the zero-offset. This indicates that the rupture bursts in the forward rupture direction after it passes by each asperity (high strain energy release zone), but the rupture velocity acceleration is not co-located with the location of asperities while high peak slip rate areas roughly coincide with the location of asperities.

It would be interesting to investigate the effect of the offset on near-field ground motion characteristics, in particular, regarding the rupture directivity effect. Also we can see that the 2D spatial coherence is a critical analysis tool in earthquake rupture since the clear pattern of spatial coherence between slip and rupture velocity, observed in the 2D analysis (Figure 4.3, top panel), is not captured in the 1D case (Figure 4.2, blue line). Lastly it is interesting to note that rise time has a negative correlation with slip, almost exactly opposite to the coherence between slip and peak slip rate (Figure 4.2). But we need to be careful in interpreting this pattern. As we see in Figure 4.4, rise time in the background area is not stably constrained. The slip weakening friction law is used in the modeling without any distinctive healing scheme. So it is not clear how to handle the multiple slipping in the background region. As we mentioned earlier, the main disadvantage of dynamic models is the lack of information to realistically parameterize the friction model and the state of stress. We may improve the situation by exploring more realistic rupture models. The negative correlation between slip and rise time observed in this analysis needs to be treated with caution for this reason. However it is encouraging that we see clear patterns of spatial coherence in both kinematic and dynamic rupture models.

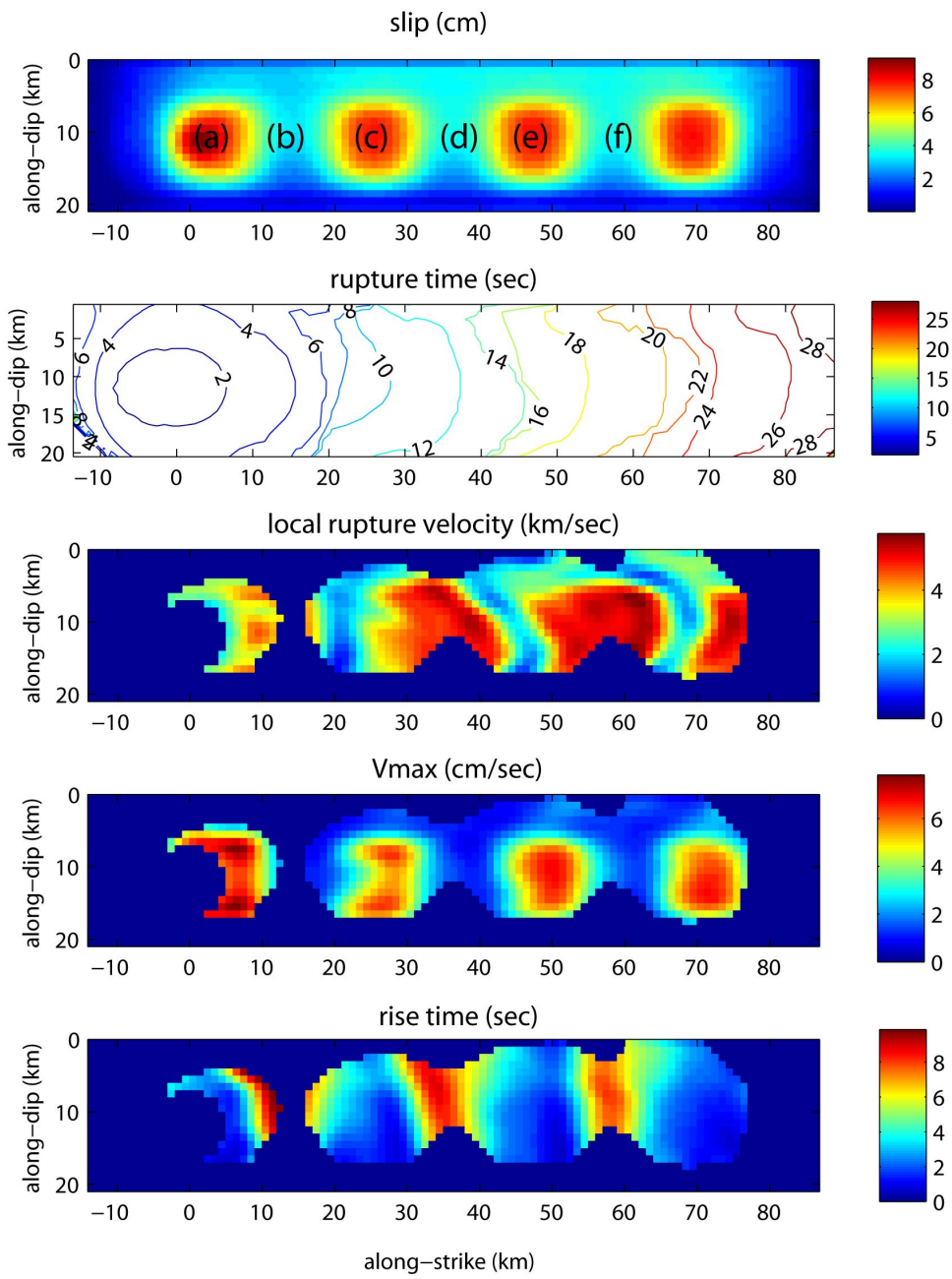

Figure 4.1. Source parameters extracted from a synthetic dynamic rupture model (Dalguer et al., 2008). The fault has 4 square-shaped asperities in a long and thin rupture area. Initial nucleation zones and small slip areas are excluded in the analysis as indicated in dark blue in the three temporal source parameters. We can visually see that the rupture bursts into the forward rupture direction if it passes by each asperity and high peak slip rate roughly coincides with the location of asperities.

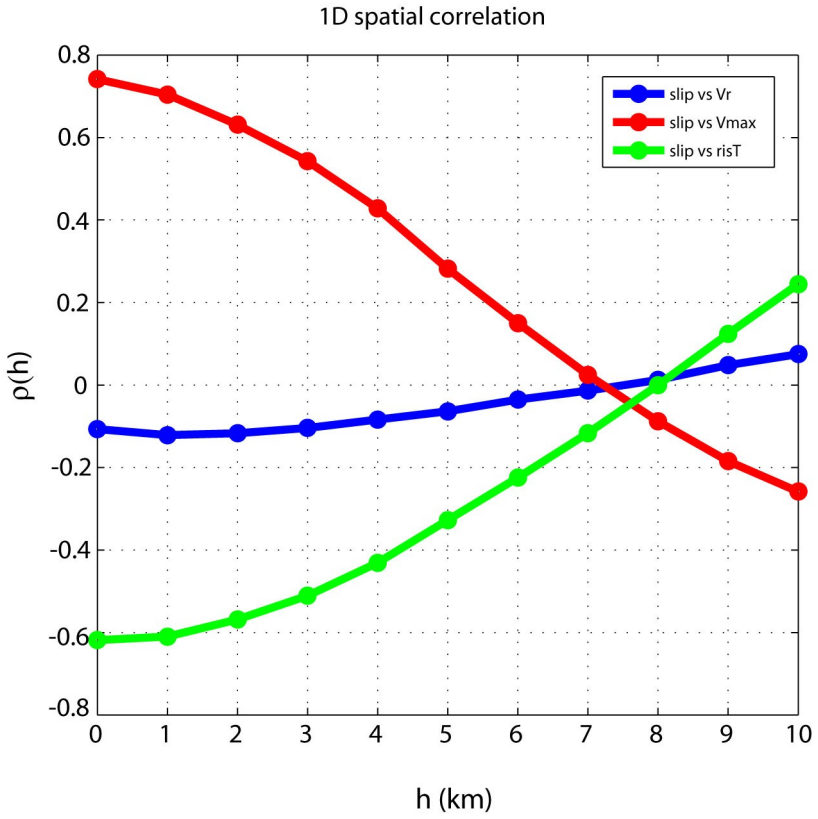

Figure 4.2. 1D spatial coherence between slip and temporal source parameters. The rupture velocity shows no significant correlation with slip in this plot while peak slip rate has strong correlation with slip. See the text for the appropriate interpretation of the negative coherence between slip and rise time.

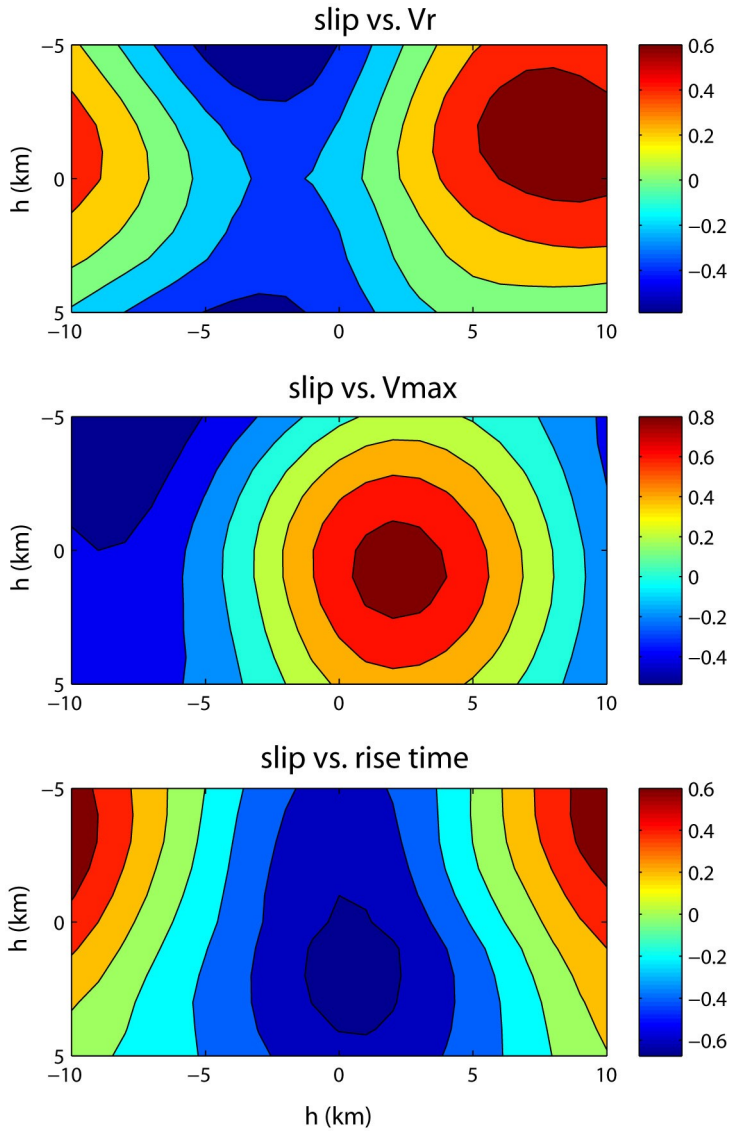

Figure 4.3. 2D spatial coherence. The correlation maximum between slip and rupture velocity is shifted about 8 km in the forward rupture direction and a clear coherence is observed in that region although no significant coherence is observed in the 1D plot (Figure 4.2). The correlation maximum between slip and peak slip rate is located near zero offset compared to that between slip and rupture velocity although there is a slight shift in the forward rupture direction (~ 2 km). The decay of coherence is not elongated in one direction as we see in the kinematic rupture models.

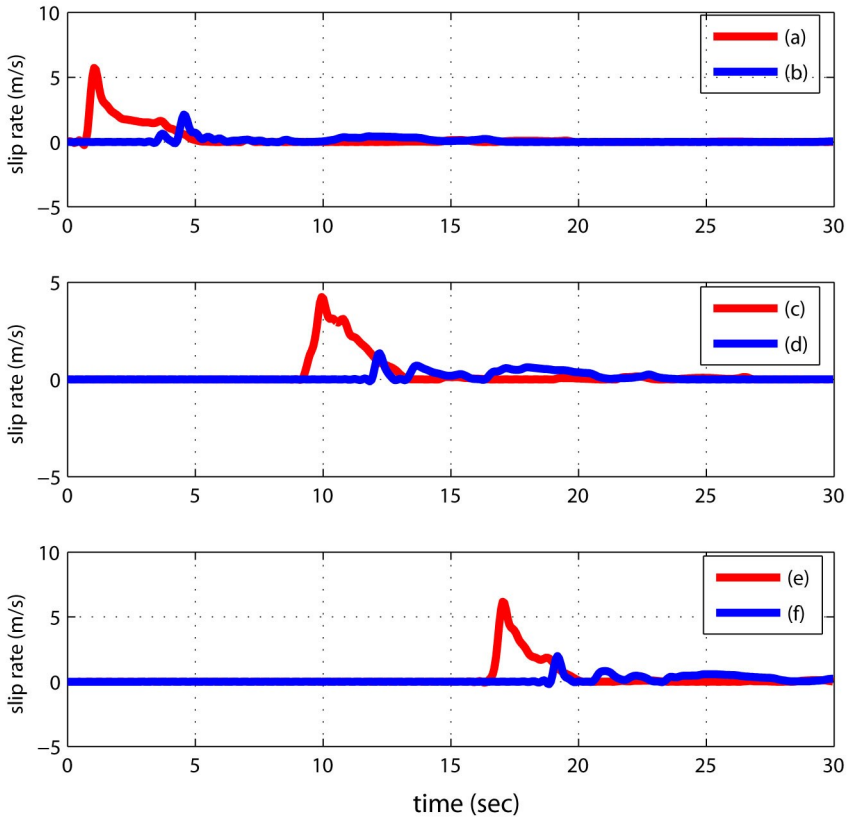

Figure 4.4. Slip velocity functions at several selected points as shown in Figure 4.1. Red and blue lines indicate SVFs within asperities and in background areas, respectively.

5. Discussion and Conclusions

One strength of the kinematic models is that they are constrained by data, but their spatial resolution is limited and their reliability has been questioned (e.q., Beresnev, 2003). We also see two different types of spatial coherence for a single event in our analysis. On the other hand, the dynamic models are obtained by spontaneous rupture modeling, so the resulting kinematic motions should be compatible with all mechanical conditions required by the governing elasto-dynamic equations. However, it also suffers from our lack of our knowledge of the stress field and frictional behavior on a fault. It is, however, encouraging that we observe clear patterns of spatial coherence both in kinematic and dynamic rupture models in this study. By taking advantage of the strengths of both kinematic and dynamic rupture models, we may reach a better understanding of earthquake source characteristics, in

particular, the interactions of source parameters in a 2D spatial domain.

Our primary goal in this study is to examine the long range variability and coherence of spatial data because of the limited resolution we have in available rupture models. Since available kinematic rupture models are not directly measured, but estimated using various inversion methods, both smoothing and regularization in the inversion and any prior specifications of model parameters can distort the true variability and continuity of the resulting spatial models. We performed low-pass filtering to remove artificial short-range variabilities that may exist in the analyzed rupture models, but we need to be careful in interpreting the resulting coherence patterns regarding the limited spatial resolution. It might be helpful to perform some synthetic tests in future works. For example, we could derive an initial (true) rupture model on a fault and ground motions on the ground, using a spontaneous dynamic rupture modeling, and carry out finite source inversion by inverting the synthetic ground motions. By testing how the estimated models are distorted by the inversion compared to the true one in terms of their spatial coherence, we may gain insight into how to interpret spatial coherence obtained from available kinematic rupture models.

We assumed stationarity for all distributions of earthquake source parameters in this study. Statistically, the random vector X(***u***) is said to be stationary within *A* (rupture area of interest) if the multivariate cumulative density function (cdf) is invariant under translation (*Goovaerts*, 1997).

$$F(\mathbf{u}_1, \ldots, \mathbf{u}_N) \;=\; F(\mathbf{u}_1+\mathbf{h}, \ldots, \mathbf{u}_N+\mathbf{h}), \quad \forall\ \mathbf{u}_1, \ldots, \mathbf{u}_N \text{ and } \mathbf{h} \tag{5.1}$$

In practice, the decision of stationarity is normally limited to one- and two-point statistics with the first two moments of the random vector as shown below.

$$E\{X(\mathbf{u}+\mathbf{h})\} \;=\; E\{X(\mathbf{u})\} \;=\; m, \quad \forall \mathbf{u} \text{ and } \mathbf{h} \tag{5.2}$$

$$C\{X(\mathbf{u}_1), X(\mathbf{u}_2)\} \;=\; C\{X(\mathbf{u}_1+\mathbf{h}), X(\mathbf{u}_2+\mathbf{h})\}, \quad \forall \mathbf{u}_1, \mathbf{u}_2 \text{ and } \mathbf{h}$$

In geoscience, the stationarity assumption can be easily violated depending on information we have in different situations. For example, if we know the probable location of asperities for an impending earthquake rupture, we may not be able to apply the simple stationary assumption we used in this study. But as pointed out by *Goovaerts* (1997), "the stationarity is not a

characteristic of the phenomenon under study, but is a decision made by the user, not a hypothesis that can be proven or refuted from data." For that reason, we think it is a viable assumption since our goal is to extract consistent features of spatial coherence between earthquake source parameters that may be embedded in earthquake rupture in general.

A correlation coefficient basically represents the linear dependency between two variables. Although two variables are directly related, the linear correlation could be small if the relation is a more complex function. Correlations between key source parameters (slip, rupture velocity, rise time, etc.) are potentially valuable and useful information for engineering practice if they can be used in earthquake source modeling. But relations between kinematic source parameters can be more complex, which can not be easily detected by a one-to-one linear dependency. Also other effects like fault geometry can be dominant in certain types of earthquake rupture. However, it is encouraging that significant correlations are observed between these key source parameters at least in the long range (low wave-number) distribution for large events. We investigated spatial coherence only between slip and temporal source parameters since slip is the best constrained source parameter and also a base parameter in earthquake source modeling. But it is also possible to look at correlations between other source parameters, for instance, between rupture velocity and peak slip rate.

The coherence analysis of well-constrained rupture models for two large strike-slip events and one synthetic spontaneous dynamic rupture model clearly shows that a significant level of correlation exists between earthquake source parameters, not only at zero offset, but in neighboring areas. By considering the neighboring areas as well as same-point correlations, many interesting features of earthquake rupture ingrained in the 2D spatial domain can be captured in the framework of spatial coherence. This new spatial coherence analysis method will help us to handle constructive and destructive interference in dynamic wave-fields, and consequently understand upper bound limits of ground motions. It may also have potential for developing effective earthquake source modeling tools in the framework of spatial coherence for realistic near-field ground motion prediction.

6. Future Work

We investigated spatial coherence between slip and temporal earthquake source parameters, including rupture velocity (Vr), peak slip rate (Vmax), and rise time (rT), in this project for a limited number of kinematic and dynamic rupture models. Our final goal, however, is to fill out all elements in the covariance matrix, shown in Figure 6.1, with consistent patterns of the spatial coherence between earthquake source parameters by examining the extended set of earthquake rupture models. The pink block in Figure 6.1 shows the spatial variability and continuity of earthquake slip and it has been extensively studied by numerous researchers, in particular, in terms of spectral decay rate in the Fourier domain (Andrews, 1980; *Herrero and Bernard*, 1994; *Somerville et al.*, 1999; *Mai and Beroza*, 2002; *Lavallée and Archuleta*, 2003). Three yellow blocks listed at the top of the matrix were explored in this study with both kinematic and dynamic rupture models. These elements link slip with the three temporal source parameters and prevent their arbitrary combination. We also need to fill out remaining

gray blocks with further study. Once we have completed the construction of the covariance matrix to indicate the spatial variability and continuity of each source parameter and spatial coherence between different source parameters, we can apply them to generating realistic earthquake source models with random sampling methods (*Goovaerts*, 1997; *Deutsch and Journel*, 1998). In this way we can produce physically self-consistent earthquake source models, including temporal source parameters. $\boldsymbol{X}=[X_1, X_2, ...]$ is a random vector composed of the source parameters of interest. If we assume that $\boldsymbol{X}$ is jointly normally distributed, we can perform multiple realizations of earthquake source models following the distribution given below.

$$\boldsymbol{X} \sim N(\boldsymbol{m}, \boldsymbol{\Sigma}) \tag{6.1}$$

$\boldsymbol{m}$ is a mean vector of the random vector, $\boldsymbol{X}$, and $\boldsymbol{\Sigma}$ is its covariance matrix.

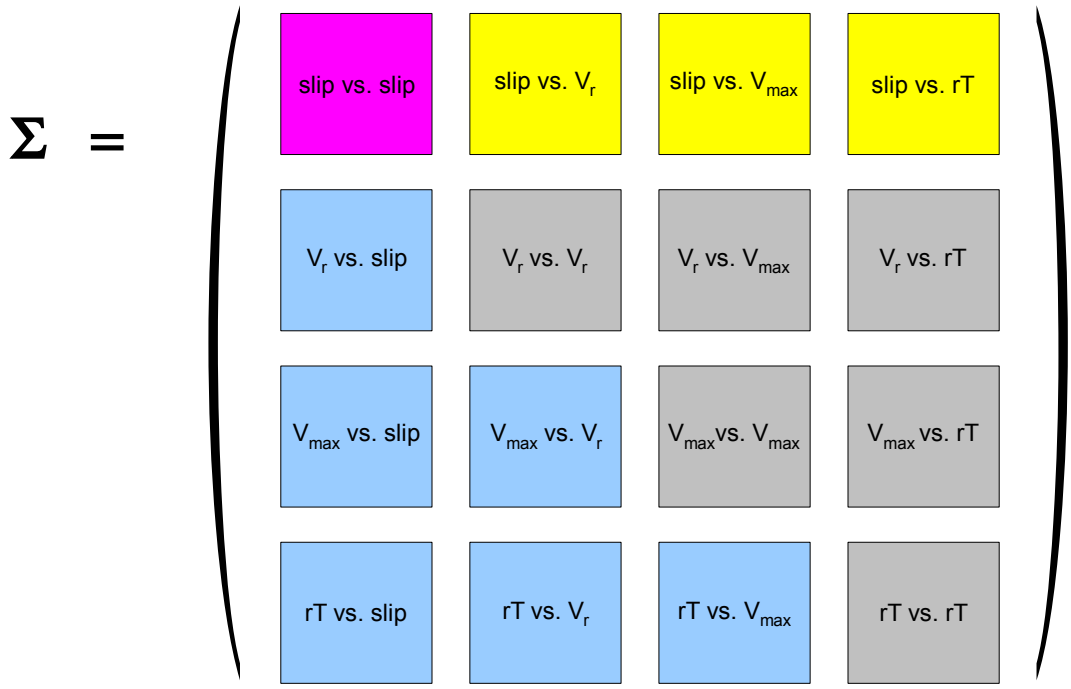

Figure 6.1. Covariance matrix (**Σ**) of a random vector, X(**u**), which contains the variability and continuity (diagonal blocks) of 4 key earthquake source parameters and their spatial coherence (off-diagonal blocks) between different parameters as well. The pink block represents the variability and continuity of earthquake slip, which has been extensively studied by numerous researchers, in particular, in terms of spectral decay rate in the Fourier domain. The three yellow blocks at the top of the matrix are investigated in this study. The gray blocks should also be examined in future work.

7. REFERENCES

Andrews, D. J., Rupture velocity of plane strain shear cracks, *J. Geophys. Res*. **81**, 5,679-5,687, 1976.

Andrews, D. J., A stochastic fault model: I. Static case, *J. Geophys. Res.*, **85**, 3,867-3,877, 1980.

Beresnev, I. A., Uncertainties in finite-fault slip inversions: To what extent to believe? (A critical review), *Bull. Seism. Soc. Am*. **93**, 2,445-2,458, 2003.

Bouchon, M., M. N. Toksöz, H. Karabulut, M. Bouin, M. Dietrich, M. Aktar, and M. Edie, Space and time evolution of rupture and faulting during the 1999 İzmit (Turkey) earthquake, *Bull. Seism. Soc. Am*. **92**, 256-266, 2002.

Dalguer, L. A., H. Miyake, S. M. Day, and K. Irikura, Surface rupturing and buried dynamic-

rupture models calibrated with statistical observations of past earthquakes, *Bull. Seism. Soc. Am*. **98**, 1,147-1,161, 2008.

Day, S. M., Three-dimensional simulation of spontaneous rupture: the effect of nonuniform prestress, *Bull. Seism. Soc. Am*. **72**, 1,881-1,902, 1982.

Delouis, B., D. Giardini, P. Lundgren, and J. Salichon, Joint inversion of InSAR, GPS, teleseismic, and strong-motion data for the spatial and temporal distribution of earthquake slip: application to the 1999 İzmit mainshock, *Bull. Seism. Soc. Am*. **92**, 278-299, 2002.

Deutsch, C. V., and A. G. Journel, *GSLIB: Geostatistical Software Library and User's Guide*, Oxford University Press, New York, 1998.

Goovaerts, P., *Geostatistics for Natural Resources Evaluation (Applied Geostatistics Series)*, Oxford University Press, New York, 1997.

Guatteri, M., P. M. Mai, and G. C. Beroza, A Pseudo-dynamic approximation to dynamic rupture models for strong ground motion prediction, *Bull. Seism. Soc. Am*. **94**, 2,051-2,063, 2004.

Hernandez, B., F. Cotton, and M. Campillo, Contribution of radar interferometry to a two-step inversion of the kinematic process of the 1992 Landers earthquake, *J. Geophys. Res*. **104**, 13,083-13,099, 1999.

Herrero, A., and P. Bernard, A kinematic self-similar rupture process for earthquakes, *Bull. Seism. Soc. Am*. **84**, 1,216-1228, 1994.

Lavallée, D., and R. J. Archuleta, Stochastic modeling of slip spatial complexities for the 1979 Imperial Valley, California, earthquake, *Geophys. Res. Lett*., **30**, 1245. doi:10.1029/2002GL015839, 2003.

Liu, P., R. J. Archuleta, and S. H. Hartzell, Prediction of broadband ground-motion time histories: hybrid low/high frequency method with correlated random source parameters, *Bull. Seism. Soc. Am*. **96**, 2,118-2,130, 2006.

Mai, P. M., and G. C. Beroza, A spatial random field model to characterize complexity in earthquake slip, *J. Geophys. Res.* **107**, 2308, doi:10.1029/2001JB000588, 2002.

Mai, P. M., J. Burjanek, B. Delouis, G. Festa, C. Francois-Holden, D. Monelli, T. Uchide, and J. Zahradnik, Earthquake source inversion blindtest: Initial results and further developments, *Eos Trans*. AGU, 88(52), Fall Meet. Suppl., Abstract S53C-08, 2007.

Somerville, P., K. Irikura, R. Graves, S. Sawada, D. Wald, N. Abrahamson, Y. Iwasaki, T. Kagawa, N. Smith, and A. Kowada, Characterizing crustal earthquake slip model for the prediction of strong ground motion, *Seismol. Res. Lett.* **70**, 59-80, 1999.

Song, S., A. Pitarka, and G. C. Beroza, Pseudo-dynamic modeling of large strike-slip earthquakes, SCEC Annual Meeting, Palm Springs, California, 2007.

Wald, D. J., and T. H. Heaton, Spatial and temporal distribution of slip for the 1992 landers, California, earthquake, *Bull. Seism. Soc. Am*. **84**, 668-691, 1994.